Highly selective and clean synthesis of nopol over well-ordered mesoporous tin silicate catalysts

M. Selvaraj*[a] and P. K. Sinha[b]

Received (in Victoria, Australia) 31st January 2010, Accepted 23rd March 2010
DOI: 10.1039/c0nj00080a

Two-dimensional SnSBA-15(CVD) catalyst was synthesized by the chemical vapor deposition (CVD) method using calcined SBA-15 with anhydrous tin(IV) chloride. For comparison studies, two mesoporous tin silicate catalysts, Sn/SBA-15(SC) and Sn/SBA-15(SA) were synthesized under the incipient wetness impregnation (IWI) method using calcined SBA-15 with different tin sources. SnMCM-41(40) was also synthesized by basic hydrothermal conditions. The synthesized mesoporous catalysts were characterized by ICP-AES, XRD, N_2 adsorption, UV vis DRS, ^{29}Si MAS NMR, FE-SEM and TEM for the proof of standard mesoporous catalysts with nature of tin on the silica pore walls. For highly selective synthesis of nopol (N–OH), the Prins condensation of β-pinene (PE) with paraformaldehyde (PF-CHO) was performed over different mesoporous catalysts such as SiSBA-15, SnSBA-15(CVD), Sn/SBA-15(SC), SnSBA-15(SA) and SnMCM-41(40), and it was conducted using a variety of optimal parameters such as amount of catalyst, reaction time, reaction temperature, ratios of reactant (PE/PF-CHO), solvents and recycles. In addition, SnSBA-15(CVD) was used in the Prins condensation of PE with PF-CHO in the presence of propyl cyanide (PrCN) with water to investigate its catalytic activity. On the basis of all catalytic results, SnSBA-15(CVD) is found to be a highly active, water-resistant and recyclable heterogeneous catalyst for selective synthesis of N–OH.

1. Introduction

Terpenes are highly useful materials in the synthesis of a variety of products such as food additives, pharmaceuticals, agrochemicals and aromas. Nopol (N–OH) is an optically active bicyclic primary alcohol used in the agrochemical industry to produce pesticides and also in the manufacture of soaps, detergents, polishes and other household products.[1] In 1946, three general methods were extensively used, as reported by Bain, in the production of N–OH by Prins condensation of β-pinene (PE) and paraformaldehyde (PF-CHO) using (i) zinc chloride as catalyst at 115–120 °C for several hours (57% yield of N–OH), (ii) acetic acid as catalyst at 120 °C which yields nopyl acetate which is then saponified to N–OH and (iii) autoclaving a mixture of PE and PF-CHO at 150–230 °C for several hours yielding quantitative amounts of N–OH.[2] However, monocyclic isomers and other side products form along with N–OH in the above methods. Generally, to decrease the selectivity of side products in several catalytic reactions, mesoporous heterogeneous catalysts have been greatly used in the production of large amounts of organic fine chemicals.[3,4]

Mesoporous MCM-41 molecular sieves synthesized with uniform pore size and an extremely high surface area have received attention from researchers in the past decade because of their potential applications as catalysts and adsorbents for large organic molecules and guest-host chemical supports.[3–7] Unfortunately, the acid strength of MCM-41 resembles that of amorphous silica aluminas rather than that of the more strongly acidic zeolites,[5] while their hydrothermal and thermal stabilities are very low due to the thin pore walls. Although the mesoporous materials are valuable for many organic conversions,[5] enhancement of the acidity is desirable for the extension of their applicability. For example, recently, Selvaraj *et al.* have reported the details of synthesis and characterization of some mesoporous materials with increasing acid strength along with enhanced hydrothermal stability, and the synthesized materials are used as catalysts for the synthesis of fine chemicals.[8–11] A few researchers reported the synthesis, characterization and catalytic applications of SnMCM-41.[12–18]

The Sn(IV) Lewis acid centers incorporated into MCM-41 catalysts, as reported by Corma *et al.*,[15–17] is used in the Baeyer–Villiger oxidation of ketones with hydrogen peroxide, and it can be also used for the synthesis of N–OH.[19] SnMCM-41 catalysts prepared using the chemical vapor deposition (CVD) method are used in the Prins condensation of PE with PF-CHO to obtain N–OH with a good selectivity.[20] Mesoporous iron phosphate prepared by direct hydrothermal method is also used in the Prins condensation reaction for the synthesis of N–OH.[21] This catalytic reaction conducted with different solvents is given a higher selectivity of N–OH with a good conversion of PE.[21] Well-ordered ZnAlMCM-41 catalysts synthesized using basic direct hydrothermal conditions were used in the Prins condensation reaction for selective synthesis of N–OH[22,23] and they gave higher selectivity of N–OH than microporous catalysts.[23] However, a few reports are available for the highly selective synthesis of N–OH over mesoporous catalysts.[19–23]

---

[a] *School of Chemical and Biomolecular Engineering, Pusan National University, Busan 609735, Korea. E-mail: chems@pnu.edu; Fax: +82-51-512-8563; Tel: +82-51-510-2397*
[b] *CWMF, BARC Facilities, Government of India, Kalpakkam, 603102, India*

In 1998, Zhao *et al.* discovered the mesoporous SBA-15 molecular sieve that was newly synthesized with tunable uniform hexagonal channels ranging from 5 to 30 nm.[24] The SBA-15 mesoporous materials have thicker framework walls than MCM-41 and also have higher hydrothermal and thermal stabilities than MCM-41. This evidence strongly suggests a better conclusion as the higher metal species can be incorporated on the surface pore walls for the introduction of catalytic active sites. However, the pure SBA-15 having acidity is not enough for increasing the catalytic activity in suitable catalytic reactions. On the basis of a serious of limitation, the mesoporous MSBA-15 (M = metal species) materials synthesized under different hydrothermal conditions were reported by several catalytic scientists. It was also found that the MSBA-15 mesoporous materials have high active sites on the silica pore walls from the observation of their characterization results. The MSBA-15 materials have been widely used as the catalysts in the several catalytic applications.[25–27] Particularly, Selvaraj and his research group successfully reported the mesoporous MSBA-15 materials (M = Cr, Mn, Sn, Ti, Ga, Al and Nb) synthesized using pH-adjusting direct hydrothermal (pH-aDH) method. From these characterization results, one can clearly conclude that MSBA-15 catalysts have higher hydrothermal stabilities than MMCM-41 catalysts. The MSBA-15 catalysts were used in different catalytic reactions to produce the selective fine chemicals.[28–35] Very recently, Selvaraj and Choe extensively reported the selective synthesis of N–OH over SnSBA-15 synthesized using pH-aDH method.[36]

In recent years, environmental and economic considerations have promoted process innovation toward cleaner technologies. Therefore, there is a great challenge to use heterogeneous catalysts that can perform under milder reaction conditions, *i.e.* lower temperatures and pressures, and which avoid the use of noxious substances and the generation of toxic waste. In this regard, to the best of our knowledge in open literature so far, SnSBA-15 synthesized by the CVD method has not been used in the Prins condensation of PE with PE-CHO for the highly selective synthesis of N–OH.

Herein we report the SnSBA-15 catalysts synthesized by different synthesis methods, and the mesoporous SnSBA-15 catalysts were used in the Prins condensation of PE with PF-CHO under liquid phase reaction conditions for the selective synthesis of N–OH. The Prins condensation reaction was carried out with different reaction parameters, *viz.* amount of catalyst, temperature, time, ratios of reactant (PE/PF-CHO), solvents and recycles. For the investigation of catalytic activity, this catalytic reaction was carried out in the presence of propyl cyanide with water. The catalytic results of SnSBA-15(CVD) for selective synthesis of nopol were also correlated and compared with other mesoporous catalysts such as SiSBA-15, Sn/SBA-15(SC), Sn/SBA-15(SA) and SnMCM-41(40).

2. Experimental section

2.1 Materials

All chemicals for the syntheses of tin-containing mesoporous catalytic materials, *viz.* triblock copolymer poly(ethylene glycol)-*block*-poly(propylene glycol)-*block*-poly(ethylene glycol) (Pluronic P123, molecular weight = 5800, $EO_{20}PO_{70}EO_{20}$), cetyltrimethylammonium bromide (CTMABr), tetraethylorthosilicate (TEOS), sodium metasilicate, hydrochloric acid (HCl), ethanol, anhydrous tin(IV) chloride ($SnCl_4$), tin(IV) chloride pentahydrate (SC) and tin(IV) acetate (SA), were purchased from Aldrich Chemical Inc. All chemicals were used as received without further purification. Millipore water was used in all experiments.

All chemicals for the synthesis of N–OH, *viz.* P-OH, PF-CHO, toluene (TMe), acetone (ACO), acetonitrile (MeCN), methanol (MeOH), *n*-butyronitrile (PrCN), *t*-butanol (*t*-BuOH), ethyl acetate (EA) and methyl ethyl ketone (MEK), were also purchased from Aldrich Chemical Inc. and used as received without further purification.

2.2 Synthesis of SnSBA-15(CVD)

The mesoporous SiSBA-15 molecular sieve has been synthesized under pH-aDH method according to the published procedure.[28] The mesoporous SnSBA-15 molecular sieve was synthesized under CVD method with very safety control. For the synthesis of SnSBA-15, 1 g of SBA-15 was exposed to the vapor produced by 1.45 ml $SnCl_4$ at 373 K in a Teflon-lined SS autoclave under autogenous pressure. After 10 h, the sample was removed from the autoclave and washed thoroughly with deionized water, and the sample was dried at 373 K and calcined at 813 K for 6 h for getting the pure solid SnSBA-15, which was denoted as SnSBA-15(CVD).

2.3 Synthesis of Sn/SBA-15(SC) and Sn/SBA-15(SA)

For comparison studies, the mesoporous Sn/SBA-15 molecular sieve was synthesized using an incipient wetness impregnation (IWI) method. In a typical synthesis, 1 g of SBA-15 dispersed in 20 ml of ethanol and a solution of SC (n_{Si}/n_{Sn} = 30) in ethanol solution were added in a round bottom flask. The mixture was stirred at 313 K under refluxing condition for 24 h and calcined in air at 813 K for 6 h to obtain Sn/SBA-15, which was denoted as Sn/SBA-15(SC). The mesoporous Sn/SBA-15 molecular sieve was synthesized using 1 g of SBA-15 with a solution of SA (n_{Si}/n_{Sn} = 30, SA was dissolved with appropriate amount of dilute HCl solution) as a tin precursor under the above similar procedure. The synthesized catalyst was denoted as Sn/SBA-15(SA).

2.4 Synthesis of SnMCM-41(40)

For comparison studies, mesoporous SnMCM-41(40) catalyst was synthesized under hydrothermal condition using cetyltrimethylammonium bromide as template with a molar ratio, 1 SiO_2/0.025 SnO_2/0.25 CTMABr/100 H_2O and characterized according to the previous published procedure.[13]

2.5 Characterization

The synthesized tin species containing mesoporous catalysts were characterized using several sophisticated instrumental techniques. The elemental compositions in the solid products were analyzed by inductively coupled plasma atomic emission spectrometry (ICP-AES, Perkin Elmer, Optima 3000). The X-ray diffraction (XRD) patterns for the samples were recorded under ambient conditions on a Shimadzu XRD-6000 with Cu Kα radiation (λ = 1.5406 Å). The sizes of the hexagonal unit cell a_0 were calculated using the formula $a_0 = 2d_{100}/\sqrt{3}$ from the d-spacing values which were calculated using the formula $n\lambda = 2d\sin\theta$. Nitrogen adsorption/desorption measurements for the catalysts were conducted using a Quantachrome Autosorb-1 by N_2 physisorption at 77 K. All catalytic samples were outgassed for 3 h at 523 K under vacuum ($p < 10^{-5}$ mbar) in the degas port of the sorption analyzer. The specific surface areas of the samples were calculated using BET method. The pore size distributions were calculated using the thermodynamic-based Barrett–Joyner–Halenda (BJH) method. The total pore volume was determined from the adsorption branch of the N_2 isotherm. The pore wall thickness (t_w) was also calculated from the unit cell parameter (a_0) and pore diameter (d_p). UV-visible diffuse reflectance (UV-vis-DR) spectra for the samples were recorded using a Perkin-Elmer Lambda 9 spectrometer. For the nuclear magnetic resonance (NMR) spectroscopic studies, the ^{29}Si MAS-NMR spectra were recorded at frequency of 59.627 MHz and a spinning rate of 2.5 kHz in a Brucker double-air bearing probes with a pulse length of 4 μs, a pulse interval of 8 s and approximately 8000 scans. TEOS (d = 82.4 ppm from tetramethylsilane (TMS)) was used as the reference compound for ^{29}Si nuclei. Field-emission scanning electron microscopy (FE-SEM) images for the samples were obtained with a JEOL JSM-6700F microscope at an accelerating voltage of 5.0 kV. Transmission electron microscopy (TEM) images for the samples were collected on a JEOL 2010 electron microscope operated at an acceleration voltage of 200 kV.

2.6 Prins condensation reaction

The Prins Condensation reaction for the synthesis of N–OH was performed in a vigorous stirring thermostated glass vessel reactor using the required amount of the desired reactants, *viz.* PE and PF-CHO in presence of a solvent (*e.g.* TMe) with an appropriate amount of tin-containing mesoporous silica catalyst under different optimal conditions. After the reaction, the mixture was extracted with acetone and analyzed by a gas chromatography (GC) with authentic samples. The major product of N–OH was again confirmed by a Hewlett-Packard 6890 Gas Chromatograph using an HP-Innowax polyethylene glycol capillary column (30 m × 320 μm × 0.25 μm) and a quadrupole mass spectrometer equipped with HP 5973 mass-selective detector. Very trace amounts of byproducts, *viz.* α-pinene, camphene and limonene, were analysed by GC with authentic samples. The conversion and selectivity were calculated using standard formulas from the GC results.

3. Results and discussion

The synthesized catalysts, *viz.* SnSBA-15(CVD), Sn/SBA-15(SC) and Sn/SBA-15(SA) have been used in the Prins condensation of PE with PF-CHO for the selective synthesis of N–OH.

3.1 SnSBA-15(CVD)

ICP-AES result for SnSBA-15(CVD) shows that the high amounts of tin content (*ca.* 0.18 wt%) have been successfully incorporated on the pore walls of SBA-15. The XRD pattern of SnSBA-15(CVD) exhibits five well-resolved peaks which are indexed to the (100), (110), (200), (210), and (300) reflections of the hexagonal *p6mm* space group (Fig. 1(a)). The observed results of d-spacing and unit cell parameter (Table 1) are well-matched with the hexagonal *p6mm* space group.[24] Additionally, the size of unit cell of SnSBA-15(CVD) is higher than that of SiSBA-15 because of Sn-ion incorporated into silica pore walls. Moreover, ionic radius of tin (69 pm) is larger than that of silicon (40 pm), and the length of Sn–O bond is greater than that of Si–O bond.[28] However, the textural properties such as pore diameter and surface area (Fig. 2(a)) of SnSBA-15(CVD) decrease as compared to those of SBA-15 but the pore wall thickness of SnSBA-15(CVD) increases as compared to that of SBA-15 (Table 1) when the Sn-ions content are increased on the surface pore walls of SBA-15. This evidence strongly supports that most of tin species are incorporated on the silica pore walls of SBA-15. A sharp UV-vis DR peak showed at 213 nm with high intensity for calcined SnSBA-15(CVD) indicates that the high amounts of tin species are incorporated on the silica pore walls with tetrahedral coordination (Fig. 3(a)). This observation result is similar to that of SnMCM-41.[12,13] Furthermore, the results of ^{29}SiMAS NMR show that the signal intensity of SnSBA-15(CVD) is much lesser than that of siliceous SBA-15 because of higher Sn substitution on the silica surface, as shown in Fig. 4; this observation clearly supports the stabilization of tin ions *via* silanol groups (defect sites).[31] TEM and FE-SEM images (Fig. 5 (a)) correspondingly show the uniform pore diameter and rope-like hexagonal mesoporous structure of SnSBA-15(CVD). The above described experimental results suggest that the "CVD method" is necessary for the large amounts of tin incorporated in the framework of silica pore walls with tetrahedral coordination.

3.2 Synthesis of Sn/SBA-15 by IWI method

The powder XRD patterns of Sn/SBA-15(SC) and Sn/SBA-15(SA) samples are shown in Fig. 1(b and c). The XRD patterns of these mesoporous materials exhibit five

Table 1 Physico-chemical properties of Sn-containing mesoporous catalysts

Sample	d_{100}/Å	a_0/Å	A_{BET}/m^2 g^{-1}	d_p/Å	V_p/cm^3 g^{-1}	$t_w = a_0 - d_p$/Å
SiSBA-15	102.4	118.2	908	87.4	1.07	30.8
SnSBA-15(CVD)	109.8	126.7	729	80.3	1.00	46.4
Sn/SBA-15(SC)	109.2	126.1	650	78.5	0.99	47.6
Sn/SBA-15(SA)	108.9	125.7	575	78.3	0.99	47.4
SnMCM-41(40)	38.6	44.57	1080	30.4	0.77	14.17

a_0, unit cell parameter; A_{BET}, specific surface area; d_p, pore diameter; V_p, pore volume; pore wall thickness (t_w) = unit cell parameter (a_0) − pore diameter (d_p).

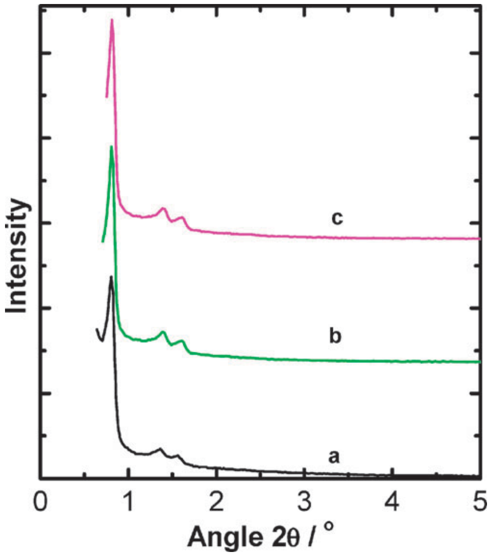

Fig. 1 XRD powder patterns of calcined (a) SnSBA-15(CVD), (b) Sn/SBA-15(SC) and (c) Sn/SBA-15(SA).

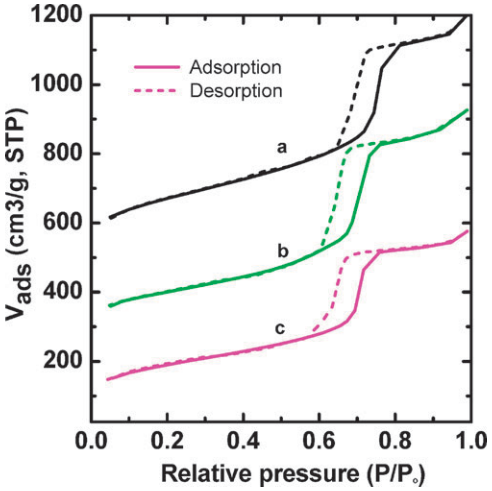

Fig. 2 Nitrogen adsorption isotherms of calcined (a) SnSBA-15(CVD), (b) Sn/SBA-15(SC) and (c) Sn/SBA-15(SA).

well-resolved peaks which are indexed to the (100), (110), (200), (210), and (300) reflections of the hexagonal *p*6*mm* space group. The observed *d*-spacing and unit cell parameter results (Table 1) are well-matched with the hexagonal *p*6*mm* space group.[24] The size of the unit cell in Sn/SBA-15(SC) is higher than that of Sn/SBA-15(SA).[31] While the broad and higher angle-XRD peak (not shown) confirms that a few amount of nanosized SnO_2 are present in the mesoporous Sn/SBA-15(SA). Moreover, ICP-AES results show that the tin content (n_{Si}/n_{Sn} = 39) in the product of Sn/SBA-15(SC) is higher compared to that (n_{Si}/n_{Sn} = 43) of Sn/SBA-15(SA), as shown in Table 1.

The N_2 adsorption–desorption isotherms of calcined Sn/SBA-15(SC) and Sn/SBA-15(SA) prepared by IWI method, are shown in Fig. 2(b and c). The textural properties of the Sn/SBA-15(SC) and Sn/SBA-15(SA) samples are given in Table 1. All isotherms are type IV according to the IUPAC classification and exhibited a H1-type broad hysteresis loop, which is typical of large-pore mesoporous solids.[37] As the relative pressure increases (p/p_0 = 0.6), all isotherms exhibit a sharp step characteristic of capillary condensation of nitrogen within uniform mesopores, where the p/p_0 position of the inflection point is correlated to the diameter of the mesopore. As SBA-15 has a hexagonal arrangement of mesopores connected by smaller micropores,[38] it is clear that the broad hysteresis loop in the isotherms of SBA-15 reflects the long mesopores which limit the emptying and filling of the accessible volume. Textural properties such as specific surface area, pore diameter and pore wall thickness of the Sn/SBA-15(SC) sample are somewhat higher than those of Sn/SBA-15(SA) because the

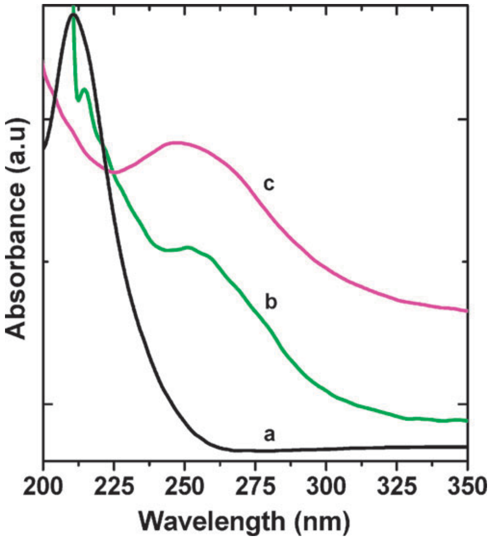

Fig. 3 UV-vis DR spectra of calcined (a) SnSBA-15(CVD), (b) Sn/SBA-15(SC), and (c) Sn/SBA-15(SA).

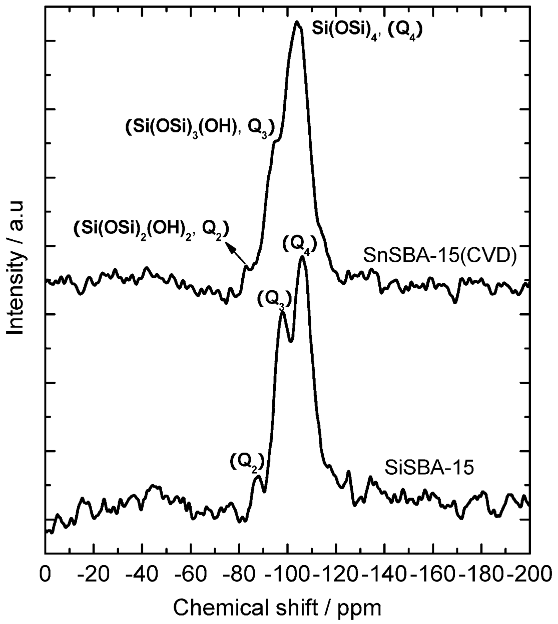

Fig. 4 ^{29}Si MAS NMR spectra of calcined SnSBA-15(CVD) and SiSBA-15.

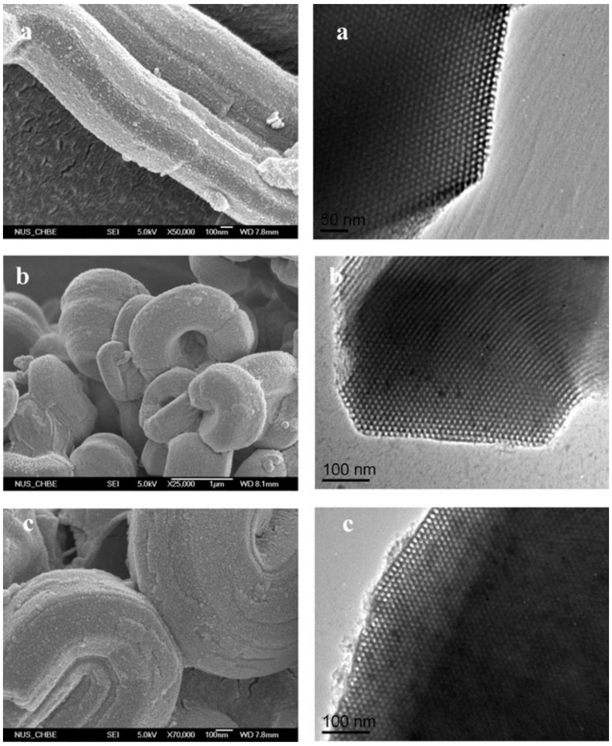

Fig. 5 SEM (left) and TEM (right) micrographs of calcined (a) SnSBA-15(CVD), (b) Sn/SBA-15(SC) and (c) Sn/SBA-15(SA).

Sn/SBA-15(SC) has higher tin species in the framework of silica walls than Sn/SBA-15(SA), as shown in Table 1. Moreover, the physicochemical characterization results of Sn/SBA-15(SC) show that the tin ions are highly incorporated on the silica pore walls using IWI method. It is also found that SC is superior tin source than SA.

For calcined Sn/SBA-15(SC), a sharp and high intensity of UV-vis DR peak (Fig. 3(b)) showed around 214 nm indicates that the most of tin species are incorporated on the silica pore walls with tetrahedral coordination, and a broad UV-vis DR peak showed at 253 nm reveals that a few amounts of tin species are incorporated into the SBA-15 with octahedral coordination. For calcined Sn/SBA-15(SA), UV-vis DR spectrum shows an absorption peak assigned at 253 nm (Fig. 3(c)). A broad and higher intensity of this absorption band indicates that tin species are highly incorporated in calcined Sn/SBA-15(SA), and that reveals the presence of Sn^{4+} in octahedral coordination. These UV-vis DR results clearly show that the "efficiency" of tin incorporation in Sn/SBA-15(SC) is higher than that of Sn/SBA-15(SA) because the counter-ion (Cl^-) of SC binds more easily with silanol group than that (CH_3COO^-) of SA, as previously reported by Selvaraj and Kawi.[31]

In the ^{29}Si MAS-NMR spectra of calcined Sn/SBA-15(SC) and Sn/SBA-15(SA), a chemical shift peak at −110 ppm is assigned to the $Si(OSi)_4$ (Q_4) sites, and other chemical shift peak at −102 ppm is attributed to the $Si–(OSi)_3OH$ (Q_3) site (not shown). The ^{29}Si MAS-NMR spectra show that intensity of Q_3 silanol groups in the both Sn/SBA-15(SC) and Sn/SBA-15(SA) is lower than that of SiSBA-15. Because the large numbers of tin species are substituted for Q_3 silanol groups. The similar effect has been found by Selvaraj and Lee when the both V and Mo species are incorporated into MCM-41 using direct hydrothermal method.[39] From these results, it is found that the Sn^{4+} species is strongly bonded in the framework of silica walls of Sn/SBA-15(SC) and Sn/SBA-15(SA).

FE-SEM images (Fig. 5b and c) show that the morphology of both Sn/SBA-15(SC) and Sn/SBA-15(SA) synthesized by IWI method, resulting in morphology like those of rope-like hexagonal mesoporous materials. The both Sn/SBA-15(SC) and Sn/SBA-15(SA) samples have long rope-like aspect of as much as several hundred micrometers those are made up of a bundle of ropes of diameter ~10 μm. It should be noted that the image in Fig. 5b and c is similar to that reported by Selvaraj and Kawi.[28]

TEM images show well-ordered hexagonal arrays of 1D mesoporous channels and further confirm that the both mesoporous materials, *viz.* Sn/SBA-15(SC) and Sn/SBA-15(SA) have 2D *p6mm* hexagonal structures (Fig. 5b and c). The average thickness of the pore walls in the mesoporous materials is *ca.* ~4.7 nm, which is much larger than that for MCM-41,[24] and the pore diameter in the samples is around ~7.8 nm, in agreement with the N_2 adsorption measurements.

Finally, the above results of ICP-AES, XRD, N_2 adsorption, UV-vis DRS and ^{29}Si MAS-NMR suggest that, the tetrahedral tin incorporated in the framework of silica walls of Sn/SBA-15(SC) by IWI method is higher as compared to that of Sn/SBA-15(SA). Although the IWI is a good method, it does not support for the incorporation of high tetrahedral tin on the silica pore walls. But, the high amounts of tetrahedral tin formed on the silica surface depend upon the tin sources. Based on the evaluation of various methods, it is clearly found that the highly ordered SnSBA-15(CVD) synthesized using CVD method has higher tetrahedral tin incorporated in the framework of silica walls than that of other Sn/SBA-15 synthesized using IWI method.

3.3 SnMCM-41

As shown in a previously published report,[13] the results of structural and textural properties of SnMCM-41 are shown in Table 1. ICP-AES result shows that the high amounts of tin content ($n_{Si}/n_{Sn} = 37.2$) have been successfully incorporated in the framework of silica walls. The studies of FTIR and UV-vis DRS confirm that the tin species are tetrahedrally coordinated on the silica pore walls of MCM-41.

3.4 Prins condensation of PE

The Prins condensation of PE was carried out with 1 : 2 mmol ratio of $n_{PE}/n_{PF\text{-}CHO}$ (4 mmol of PE and 8 mmol of PF-CHO), as the reactants and 9 ml of TMe, as a solvent at 363 K for 6 h over several catalysts, *viz.* SiSBA-15, SnSBA-15(CVD), Sn/SBA-15(SC), Sn/SBA-15(SA) and SnMCM-41(40), and the catalytic results of this reaction are shown in Table 2. The order of catalytic activity for selectivity of N–OH is found as follows: SnSBA-15(CVD) > Sn/SBA-15(SC) > Sn/SBA-15(SA) > SiSBA-15. SnSBA-15(CVD) exhibits the best performance with a conversion of PE, 100% and a selectivity of N–OH, 98.1%. Very trace amounts of selectivity of byproducts, *viz.* α-pinene, camphene and limonene, form

Table 2 Prins condensation of PE over various types of mesoporous Sn-containing mesoporous catalysts[a]

Catalysts	Conversion of PE (%)	Selectivity of N–OH (%)	TON[b]
SiSBA-15	15.4	60.0	—
SnSBA-15(CVD)	100	98.1	2638
Sn/SBA-15(SC)	96.5	87.5	2291
Sn/SBA-15(SA)	85.3	75.5	2531
Recycling 2[c]	99.8	94.3	2787
Recycling 3[c]	99.9	94.3	2790
Recycling 2[d]	90.4	80.2	2384
Recycling 3[d]	90.3	80.3	2382
Recycling 2[e]	81.4	72.3	2576
Recycling 3[e]	81.5	72.4	2579
SnMCM-41(40)	91.3	82.3	1734
Absence of catalyst	—		—

[a] *Reaction conditions*: 0.1 g of catalyst; 4 mmol of PE and 8 mmol of PF-CHO (1 : 2 mmol ratio) in the presence of 9 ml of TMe (solvent) were introduced into a reactor; reaction temperature, 363 K; reaction time, 6 h. [b] Turnover number (TON) = mole of PE converted/mol of active site. Recycling: [c] SnSBA-15(CVD), [d] Sn/SBA-15(SC) and [e] Sn/SBA-15(SA) after exhaustive washing with acetone 313 K and drying at 393 K overnight.

during the PE isomerization in the presence of weak and strong Lewis acid sites of SnSBA-15 catalysts (not shown). SnSBA-15(CVD) has higher conversion of PE and selectivity of N–OH than other SnSBA-15. The observed higher activity of SnSBA-1(5) is tentatively ascribed to its two-dimensional space and high loading of tetrahedral Sn^{4+} species on the inner pore walls of SBA-15, resulting in a higher number of accessible active sites because the Sn^{4+}-ion produces a high numbers of Lewis acid sites on the inner surface of pore walls.

Sn/SBA-15(SC) has a higher conversion of PE and selectivity of N–OH (Table 2) than Sn/SBA-15(SA) due to the higher numbers of Lewis acid sites with tetrahedral coordination. Although Sn/SBA-15(SA) has higher hexa-coordinated tin species than Sn/SBA-15(SC), its conversion of PE and selectivity of N–OH is not largely affected, because the tin-ions are acting as water-resistant Lewis acid sites on the surface of mesoporous silica, as reported by Corma *et al.*[17,19] We have clearly discussed with an experimental result in the next section.

Although SnSBA-15(CVD) has low tetrahedral tin species than SnMCM-41(40), it has significantly higher conversion of PE and selectivity of N–OH as compared to SnMCM-41(40) (Table 2) because of higher structural and textural properties than SnMCM-41(40). It is interesting to note that the well-ordered mesostructural catalyst also plays a very important catalytic role in the production of N–OH with a good selectivity. SnSBA-15(CVD) also has higher turnover number (TON, which is defined as mol of PE converted/mol of active sites) than other tin-containing silica catalysts, *viz*., Sn/SBA-15(SC), Sn/SBA-15(SA) and SnMCM-41(40). This evidence strongly supports that the high amounts of tetrahedral tin species containing SBA-15 have also good catalytic activity for this reaction. Based on the overview point, it is interestingly found that the CVD method is a good method for the synthesis of SnSBA-15 with high tetrahedral tin than IWI method.

Initially, the used mesoporous tin-containing SBA-15 catalysts (SnSBA-15(CVD), Sn/SBA-15(SC) and Sn/SBA-15(SA)) usually suffer from loss of catalytic activity, and hence the catalysts need to be regenerated by washing and thermal treatments. The recycled catalysts such as SnSBA-15(CVD), Sn/SBA-15(SC) and Sn/SBA-15(SA) were washed four times with acetone and dried at 393 K overnight in order to remove the organics and unreacted PF-CHO. No losses of the catalytic activities and tin species on the surface of catalysts are observed after three recycles. Their conversions and selectivities also remain constant after three recycles (Table 2) while the TON of these catalysts also remains constant. Especially, for the Prins condensation reaction, the SnSBA-15(CVD) is more active and suitable catalyst than other catalysts such as Sn/SBA-15(SC) and Sn/SBA-15(SA) due to greater tetrahedral tin species incorporated in the framework of silica pore walls. This reaction has also been performed in SiSBA-15, which gives a less performance of catalytic activity because of having less acid sites. The formation of N–OH is not detected when the Prins condensation reaction was carried out without

Table 3 Prins condensation of PE with different reaction parameters over SnSBA-15(CVD)[a]

S. No.	Amount of SnSBA-15(CVD) catalyst/g	Amount of TMe/ml	Conversion of PE (%)	Selectivity of N–OH (%)	TON
1	0.1	9	100	98.1	2638
2	0.15	9	100	98.6	1758
3	0.2	9	100	98.9	1319
4	0.1	5	52.3	46.3	1380
5	0.1[b]	14	67.4	62.4	1778
6	0.1[c]	9	51.2	46.5	1351
7	0.1[d]	9	60.2	53.6	3176

[a] *Reaction conditions*: reactants, 4 mmol of PE and 8 mmol of PF-CHO (1 : 2 mmol ratio); time, 6 h; [b] time, 2 h; temperature, 363 K; [c] 4 mmol of PE and 4 mmol of PF-CHO (1 : 1 mmol ratio); [d] 8 mmol of PE and 4 mmol of PF-CHO (2 : 1 mmol ratio).

catalyst (Table 2). Since SnSBA-15(CVD) is an excellent active catalyst on the catalytic reaction, it is used to find the best optimal condition for highly selective synthesis of N–OH.

To find the best optimal conditions, the Prins condensation reaction was performed over SnSBA-15(CVD) using the different optimal conditions such as amount of catalyst, reaction temperature, reaction time, ratios of reactant (PE: PF-CHO) and solvents.

The Prins condensation reaction was carried out with various amounts of SnSBA-15(CVD) catalyst using the reaction conditions noted in Table 3 (S. No. 1–3). When the amount of catalyst is varied from 0.1 to 0.2 g, the conversion of PE and selectivity of N–OH are not majorly affected but TON values decrease. This evidence strongly supports that a low tetrahedral tin containing SBA-15 is effectively suitable to get an excellent selectivity of N–OH in the similar reaction condition.

For this catalytic reaction, the amount of solvent (TMe) was also varied using the reaction conditions noted in Table 3 (S. No. 1, 4, 5). When this reaction was performed with 9 ml of TMe under the similar reaction condition, it produces the high conversion of PE, 100% and selectivity of N–OH 98.1%. However, the less conversion of PE and selectivity of N–OH are observed during this reaction with 5 ml of TMe because the PF-CHO may not be completely dissolved and reacted with PE. A very trace amounts of byproduct, *viz.* α-pinene, camphene and limonene, form during the isomerization of PE in the presence of weak or strong acid sites (not shown). Moreover, the conversion of PE and selectivity of N–OH are also less with the increase of TON when the Prins condensation reaction is carried out with 14 ml of TMe for 2 h. But, it is noteworthy that the conversion of PE (67.4%) and selectivity of N–OH (62.4%) at 2 h are better compared to those of the standard reaction. Then, the obtained results clearly show that the conversion of PE and selectivity of N–OH are not affected during this reaction with higher amount of solvent (up to 14 ml).

To find the best reactant ratio for the highly selective synthesis of N–OH, the Prins condensation reaction was performed with different mmol ratio of $n_{\mathrm{PE}}/n_{\mathrm{PF-CHO}}$ using the reaction conditions noted in Table 3 (S. No. 1, 6, 7). When the catalytic reaction is carried out with 1 : 1 and 2 : 1 mmol ratios of $n_{\mathrm{PE}}/n_{\mathrm{PF\text{-}CHO}}$, it has a lower conversion of PE and selectivity of N–OH in 1 : 1 with the decrease of TON but it produces slightly higher conversion of PE and selectivity of N–OH in 2 : 1 with the increase of TON. In these ratios, the possibly reason is the insufficient quantity of reactants to mix with each other as a homogeneous solution. Although 2 : 1 mmol ratio has higher TON than 1 : 2 mmol ratio, it gives much lesser conversion of PE and selectivity of N–OH than 1 : 2 mmol ratio. Moreover, in 1 : 2 mmol ratio the reactant mutually reacts with each other on the catalytic surface. This evidence strongly supports that 1 : 2 mmol ratio is the best ratio among the other ratios, for obtaining an excellent selectivity of N–OH.

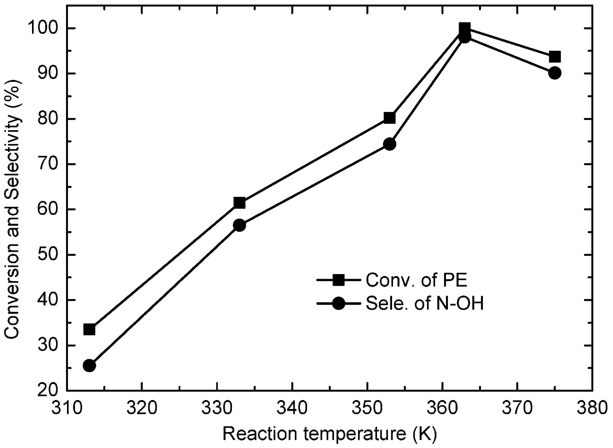

Fig. 6 Variation of temperature on the synthesis of N–OH by Prins condensation of PE with PF-CHO. *Reaction conditions*: 0.1 g of SnSBA-15(CVD) catalyst; 4 mmol of PE and 8 mmol of PF-CHO (1 : 2 mmol ratio) in the presence of 9 ml of TMe (solvent) were introduced into a reactor; reaction time, 6 h.

For the production of highly selective synthesis of N–OH, the Prins condensation reaction was carried out with various reaction temperatures using the reaction conditions noted in Fig. 6. When the reaction temperature is decreased from 363 K to 313 K, the rate of both PE consumption and N–OH formation decreases, and the less conversion of PE and selectivity of N–OH are observed with the decrease of TON. This may be due to the less activity of Lewis active sites on the surface of the catalyst at low reaction temperature, which is not supported to react with each other (reactant of PE and PF-CHO). Moreover, the conversion of PE and selectivity of N–OH also decrease with increasing the number of isomers and other side products when the reaction temperature is increased at above 370 K. This evidence strongly supports that a low (< 313 K) or high (> 370 K) reaction temperature is not favorable to produce highly selective synthesis of N–OH.

To find a suitable reaction time for the highly selective synthesis of N–OH, the Prins condensation reaction was carried using the reaction conditions noted in Fig. 7. At 3 h, the conversion of PE and selectivity of N–OH are 80.5% and 71.3%, respectively. The selectivity of N–OH increases from 80.5 to 98.1% when the reaction time is increased from

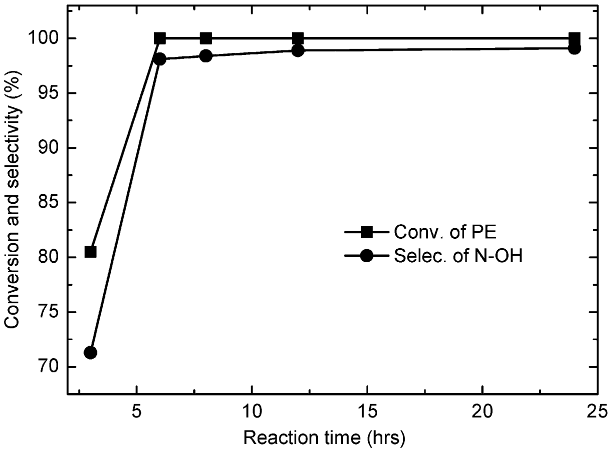

Fig. 7 Variation of time on the synthesis of N–OH by Prins condensation of PE with PF-CHO. Reaction conditions: 0.1 g of SnSBA-15 catalyst; 4 mmol of PE and 8 mmol of PF-CHO (1 : 2 mmol ratio) in the presence of 9 ml of TMe (solvent) were introduced into a reactor; reaction temperature, 363 K.

Table 4 Prins condensation of PE with different solvents over SnSBA-15(CVD)[a]

S. No.	Solvents	Temp./K	Time/h	Conversion of PE (%)	Selectivity of N–OH (%)	TON
1	MeCN	353	2	58.4	84.6	1540
2	MeOH	353	2	8.3	5.3	219
3	*t*-BuOH	353	2	40.2	81.5	1060
4	EA	353	2	78.9	71.2	2081
5	MEK	353	2	71.1	81.4	1875
6	TMe	353	2	80.3	73.5	2118
7	PrCN	363	6	95.2	81.3	2511
8	PrCN	373	8	97.3	85.3	2566
9	PrCN + 50 mg of water	373	8	93.6	89.2	2469
10	PrCN + 100 mg of water	373	8	95.8	90.2	2527
11	TMe	363	6	100	98.1	2638

[a] *Reaction conditions*: catalyst, 0.1 g of SnSBA-15(CVD); reactants, 4 mmol of PE and 8 mmol of PF-CHO (1 : 2 mmol ratio); 9 ml of solvent.

3 to 8 h. The TON of this reaction also increases with increasing the time from 3 to 8 h. When the reaction time is increased from 12 to 24 h, the conversion of PE and selectivity of N–OH are not largely varied, and also the TON value is not majorly changed. Based on the catalytic results, it is clearly observed that a low (3 h) reaction time is also good for obtaining a high conversion of PE. However, the selectivity of N–OH majorly decreases. Overall, it is concluded that optimum time is 6 h for the highly selective synthesis of N–OH.

The Prins condensation reaction was also performed with a variety of solvents, time and temperature using the reaction conditions noted in Table 4. TMe and EA are apolar aprotic solvents. When these solvents are used at 353 K and 2 h, the high conversion of PE and selectivity of N–OH are observed because of increasing the catalytic activity (S. No. 4, 6). However, TMe has higher conversion of PE and selectivity of N–OH than EA, and a few amounts of nopyl acetate form during the reaction with EA. *t*-BuOH, MEK and MeCN are dipolar solvents. when these solvents are used with 353 K and 2 h (S. No. 1, 3, 5), the conversion of PE increases in order to MEK > MeCN > *t*-BuOH, and selectivity of N–OH also increases in order to MeCN > *t*-BuOH > MEK. It might be noted that the converted PE in the both solvents, *viz*. *t*-BuOH and MeCN, is almost completely formed as N–OH, but in MEK a few amounts of byproduct form with N–OH. MeOH is a protic solvent (S. No. 2), which gives low conversion of PE and selectivity of N–OH at 353 K and 2 h because of less supporting with reactants and the surface of catalyst. When the Prins condensation reaction is conducted at 363 K and 6 h in the presence of PrCN, the conversion of PE and selectivity of N–OH are not largely changed (S. No. 7), but the increase of conversion and selectivity are observed (S. No. 8) when the reaction is carried out at higher temperature (373 K) and time (8 h). It is indicated that the catalytic activity slowly improves during the reaction with this solvent. On the basis of catalytic activity, it is clearly found that TMe is the best solvent among the other solvents (S. No. 11), for the production of high selectivity of N–OH in a low reaction time and temperature.

To investigate the stability of catalyst against water, the Prins condensation reaction was conducted with various amounts of water using the reaction conditions noted in Table 4 (S. No. 9, 10). The high conversion of PE and selectivity of N–OH are observed when the water content is increased in the range of 50–100 mg on the reaction system under the similar reaction condition. This evidence strongly shows that the catalytic activity and stability of SnSBA-15(CVD) is not affected when the Prins condensation is carried out with water content of reactant.

4. Conclusions

The SnSBA-15(CVD) catalyst synthesized using anhydrous $SnCl_4$ as tin source was used for the highly selective synthesis of N–OH, and it was successfully synthesized under CVD method with highly ordered two-dimensional mesoporous structures and high loadings of tetrahedral tin species. For comparison studies, the mesoporous tin containing catalysts such as Sn/SBA-15(SC) and Sn/SBA-15(SA) were synthesized under IWI method, and SnMCM-41(40) was also synthesized under basic hydrothermal condition. The characteristic results of XRD, N_2 adsorption, SEM and TEM show that the mesoporous tin containing SBA-15 catalysts have the two-dimensional mesoporous structures with uniformly pore structures. The studies of ICP-AES and UV-vis DRS can be observed that the SnSBA-15(CVD) synthesized by CVD method has higher tetrahedral tin species than other catalysts, *viz*. Sn/SBA-15(SC) and Sn/SBA-15(SA). The synthesized catalysts such as SiSBA-15, SnSBA-15(CVD), Sn/SBA-15(SC), Sn/SBA-15(SA) and SnMCM-41(40) were successfully used in the production of N–OH by the Prins condensation of PE with PF-CHO. SnSBA-15(CVD) has higher catalytic activity at the suitable reaction conditions (1 : 2 mmol ratio of PE to PF-CHO, 9 ml of TMe, 363 K and 6 h) than other catalysts such as SiSBA-15, Sn/SBA-15(SC), Sn/SBA-15(SA) and SnMCM-41(40). On the basis of all catalytic experimental results, SnSBA-15(CVD) is found to be a highly active, reusable, water resistant and an environmentally friendly heterogeneous catalyst for the highly selective synthesis of N–OH, and it has superior catalytic activity in the condensation reaction than other mesoporous catalysts, *viz*. SiSBA-15, Sn/SBA-15(SC), Sn/SBA-15(SA) and SnMCM-41(40).

References

1 *Kirk-Othmer Encyclopedia of Chemical Technology*, John Wiley, New York, 1997, vol. 26.
2 J. P. Bain, *J. Am. Chem. Soc.*, 1946, **68**, 638.
3 C. T. Kresge, M. E. Leonowicz, W. J. Roth, J. C. Vartuli and J. S. Beck, *Nature*, 1992, **359**, 710.

4 J. S. Beck, J. C. Vartuli, W. J. Roth, M. E. Leonowicz, C. T. Kresge, K. D. Schmitt, C. T.-W. Chu, D. H. Olson, E. W. Sheppard, S. B. McCullen, J. B. Higgins and J. L. Schlenker, *J. Am. Chem. Soc*., 1992, **114**, 10834.
5 A. Corma, *Chem. Rev*., 1997, **97**, 2373.
6 A. Sayari, *Chem. Mater*., 1996, **8**, 1840.
7 Y. J. Ying, C. P. Mehnert and M. S. Wong, *Angew. Chem., Int. Ed*., 1999, **38**, 56.
8 M. Selvaraj, A. Pandurangan, K. S. Seshadri, P. K. Sinha, V. Krishnasamy and K. B. Lal, *J. Mol. Catal. A: Chem*., 2002, **186**, 173.
9 M. Selvaraj, A. Pandurangan, K. S. Seshadri, P. K. Sinha and K. B. Lal, *Appl. Catal., A*, 2003, **242**, 347.
10 M. Selvaraj, P. K. Sinha, K. S. Seshadri and A. Pandurangan, *Appl. Catal., A*, 2004, **265**, 75.
11 M. Selvaraj and T. G. Lee, *Microporous Mesoporous Mater*., 2005, **85**, 52.
12 T. K. Das, K. Chaudhari, A. J. Chandwadkar and S. Sivasanker, *J. Chem. Soc., Chem. Commun*., 1995, 2495.
13 M. Selvaraj, B. H. Kim and T. G. Lee, *Chem. Lett*., 2005, **34**, 1290.
14 K. Chaudhari, T. K. Das, P. R. Rajmohanan, K. Lazar, S. Sivasanker and A. Chandwadkar, *J. Catal*., 1999, **183**, 281.
15 A. Corma, M. T. Navarro and M. Renz, *J. Catal*., 2003, **219**, 242.
16 A. Corma, M. T. Navarro, L. Nemeth and M. Renz, *Chem. Commun*., 2001, 2190.
17 A. Corma, S. Iborra, M. Mifsud and M. Renz, *J. Catal*., 2005, **234**, 96.
18 S. Samantha, N. K. Mal, A. Manna and A. Bhaumik, *Appl. Catal., A*, 2004, **273**, 157.
19 A. Corma and M. Renz, *ARKIVOC*, 2007, 40.
20 A. L. Villa de P, E. Alarcon and C. M. de Correa, *Chem. Commun*., 2002, 2654.
21 U. R. Pillai and E. Sahle-Demessie, *Chem. Commun*., 2004, 826.
22 M. Selvaraj, B. R. Min, Y. G. Shul and T. G. Lee, *Microporous Mesoporous Mater*., 2004, **74**, 143.
23 M. Selvaraj and S. Kawi, *J. Mol. Catal. A: Chem*., 2006, **246**, 218.
24 D. Zhao, J. Feng, Q. Huo, N. Melosh, G. H. Fredrickson, B. F. Chmelka and G. D. Stucky, *Science*, 1998, **279**, 548.
25 S. Wu, Y. Han, Y.-C. Zou, J.-W. Song, L. Zhao, Y. Di, S.-Z. Liu and F.-S. Xiao, *Chem. Mater*., 2004, **16**, 486.
26 Y. Yue, A. Gideon, J.-L. Bonardet, N. Melosh, J.-B. D'Espinose and J. Fraissard, *Chem. Commun*., 1999, 1967.
27 W.-H. Zhang, J. Lu, B. Han, M. Li, J. Xiu, P. Ying and C. Li, *Chem. Mater*., 2002, **14**, 3413.
28 M. Selvaraj and S. Kawi, *Chem. Mater*., 2007, **19**, 509; M. Selvaraj, M. Kandaswamy, D.W. Park and C. S. Ha, *Catal. Today*, 2010, in press, DOI: 10.1016/j.cattod.2010.03.061.
29 M. Selvaraj and S. Kawi, *Microporous Mesoporous Mater*., 2007, **101**, 240.
30 M. Selvaraj and T. G. Lee, *J. Phys. Chem. B*, 2006, **110**, 21793.
31 M. Selvaraj and S. Kawi, *J. Mater. Chem*., 2007, **17**, 3610; M. Selvaraj, M. Kandaswamy, D. W. Park and C. S. Ha, *Catal. Today*, 2010, in press, DOI: 10.1016/j.cattod.2010.04.041.
32 M. Selvaraj, S. Kawi, D.-W. Park and C. S. Ha, *Microporous Mesoporous Mater*., 2009, **117**, 586.
33 M. Selvaraj and S. Kawi, *Catal. Today*, 2008, **131**, 82.
34 M. Selvaraj and S. Kawi, *Stud. Surf. Sci. Catal*., 2007, **165**, 219.
35 M. Selvaraj, S. Kawi, D.-W. Park and C. S. Ha, *J. Phys. Chem. C*, 2009, **113**, 7743.
36 M. Selvaraj and Y. Choe, *Appl. Catal., A*, 2010, **373**, 186.
37 M. Kruk, M. Jaroniec and A. Sayari, *Chem. Mater*., 1999, **11**, 492.
38 M. Imperor-Clerc, P. Davidson and A. Davidson, *J. Am. Chem. Soc*., 2000, **122**, 11925.
39 M. Selvaraj and T. G. Lee, *Microporous Mesoporous Mater*., 2005, **85**, 39.